

ESTIMATES OF ACCURACY AND EFFICIENCY OF A MOM ALGORITHM IN L_2 FOR 2-D SCREENS

A. G. Tyzhnenko and Y. V. Ryznik

Department of Mathematics
Kharkiv National University
9A, Lenin Ave., 610001, Kharkiv, Ukraine

Abstract—A rigorous solution in L_2 to the EFIE for 2-D screens is developed and proposed as a reference solution for testing the convergence rate and scattering amplitude error of any MoM algorithm in L_2 . The proposed reference solution permits to choose judiciously an appropriate mesh density for a MoM algorithm instead of using the ten-points-rule in all cases. Additionally, using the reference solution it is demonstrated that the discrepancy should not be used as a performance value of the scattering amplitude error while solving the EFIE with the MoM in L_2 . Both the E - and H -cases are considered.

1. INTRODUCTION

Recently, we can observe an explicit shift in practical investigations from experimental modeling to computer simulation. In this connection, an experimentalist has the need for adequate and cheap method, which permits to provide such a simulation. Nowadays, to provide computer simulations in electromagnetics practitioners frequently use the MoM solution to boundary integral equations.

The method of moments (MoM) for solving surface integral equations in scattering problems is widely used in computational electromagnetics. At that, the appropriate 2-d kind equations can be solved without significant computational problems, but they do not applicable to screens. For these ones, first kind integral equations are frequently used in practice. The convergence problem for MoM solutions to the electric field integral equations (EFIE) was not solved for a long time until landmark works [1–5] was published. In these works, both the convergence of a MoM algorithm and the boundness of MoM matrix condition number were proved in fractional order Sobolev spaces. Unfortunately, a theoretical analysis for MoM

solutions to the first kind integral equations in the Sobolev spaces does not permit to estimate a magnitude of an actual error and hence a scattering amplitude error. Besides, the usage of an inner product in the appropriate Sobolev space leads to dramatic increasing in computational burden. This issue prevents from wide dissemination of this method. Because of that, practitioners use the MoM algorithms in the common space of square integrable functions (L_2) with preliminary extraction of edge singularities. This issue reduces significantly the computational complexity of scattering problems but in the same time causes the convergence problem of MoM algorithms in L_2 and the problem of poor conditioning of MoM matrices. Besides, the scattering amplitude error estimation problem remains unsolved.

As to the convergence problem for two-dimensional E -screens, the proved convergence of a MoM algorithm in the Sobolev space $H^{-1/2}$ ensures the convergence in L_2 because L_2 is smaller than $H^{-1/2}$. Worth noting that for H -screens, the proved convergence in $H^{1/2}$ does not ensure the convergence in L_2 because $L_2 \supset H^{1/2}$.

Additionally, in the both E - and H -cases, transition from the Sobolev space to L_2 in the moment's method gives rise to a new problem: the condition number of a MoM matrix in L_2 increases with mesh density and electrical size of the scatterer. Also remains the actual error estimation problem and hence the problem estimation of scattering amplitude errors.

Recently, some authors have pointed out the lack of investigation of these problems for the MoM algorithms in L_2 [6–10]. Because of that, the detailed investigation of solution errors for the Dirichlet and Neumann problems for closed contour and screens has been provided in these works. So, in the work [8] authors have obtained theoretical estimates of actual errors and scattering amplitude errors for closed perfectly conducting cylinder in the non-resonance case. In addition, the theoretical estimates of matrix condition number were obtained in this work. In [9], the actual and scattering amplitude errors were estimated as for a closed contour as for an open one. At that, the circular perfectly conducting cylinder and flat metal strip were considered as testing geometries. To estimate actual errors, authors used the benchmarking on the solution based on:

- The PO approach;
- The same MoM algorithm but with very high mesh density.

However, it is worthwhile to note that the PO approach has limited area of application. For example, this one cannot be used for the nose illumination of a strip. Hence, the PO solution cannot be used as a reference solution in all cases. As to the second RS used in [9], we

should note that its realization is very expensive and has not sufficient background in H -case where the convergence of a MoM algorithm in L_2 is not proven to date.

The benchmarking on canonical problems, the rigorous solutions for which are known, can be also fulfilled (see, for example, [11–13]). However, such a benchmarking is indirect, because errors obtained for test cases may not extrapolate readily to other problems, due to problem-dependent phenomena such as resonance or edge effects. Theoretical estimation of actual error of a solution as in [9] and [14], for example, is very difficult and far not in all cases applicable. It is more convenient to use a rigorous and sufficiently simple solution in L_2 valid for any geometry as a reference solution for testing more simple MoM algorithms in L_2 and many other ones ([14, 15], for example). Such a reference solution has been not found to date for the three-dimensional case. In the two-dimensional case, such solutions were constructed in [16, 17] for closed cylinders and in [18] for H -screens. In this work, we develop such a solution for E -screens.

Analogously to the H -case, we use here the Galerkin method on a complete set of trigonometric functions. This issue permits us to obtain a Fredholm algebraic equation for modal coefficients with the aid of analytical regularization and specific property of Fourier integrals. With the Fredholm matrix equation in hand, we prove the convergence of the Galerkin MoM in L_2 , the boundness of the condition number of MoM matrix, and obtain a direct estimation of an actual error, and hence, of a scattering amplitude error for smooth screens. This issue permits one to provide adequate simulations of scattering from screens for both E - and H -cases.

The proposed method gives the opportunity to simulate scattering from screens in all cases. What is peculiarly valuable in the Galerkin solution proposed is that it permits to estimate the magnitude of scattering amplitude error and the condition number of the MoM matrix is bounded. However, its algorithm is more complicated than those of commonly used in practice, and hence more expensive. Because of that, there is the need to investigate the existent MoM algorithms in L_2 with regard to their convergence rate and scattering amplitude error behavior via incidence angle, scatterer configuration and its electric size. To this end, we propose to use the developed Galerkin method as a reference solution (RS) for testing practically used MoM algorithms in L_2 for which a condition number is not bounded and actual error magnitude cannot be estimated. Benchmarking on this RS permits one to investigate as the convergence rate of any MoM algorithm as the behavior of scattering amplitude error for some specific scattering geometry at microwave frequencies. It

is worthwhile to note that any solution in the Sobolev space cannot be used as a reference solution because one cannot calculate a magnitude of an actual error of such a solution, and hence, a scattering amplitude error.

All abovementioned considerations permit us to affirm that the RS problem has been not solved to date in acceptable manner. Therefore, we propose in the paper a new solution based on the Galerkin MoM in L_2 which can be used as a reference solution. This issue permits to achieve the following results:

- To estimate the convergence rate of a MoM algorithm in L_2 for any smooth screen and arbitrary incidence angle;
- To investigate the behavior features of an actual error with mesh density or electric size of a scatterer increasing;
- To choose an optimal mesh density for a specific scattering problem instead using of the widely known rule-of-thumb that gives ten points per wavelength in all cases.

To use a novel method solution with confidence as the reference solution, one should be convinced in adequacy of such a solution. To verify this issue, we compare the novel method with convergent series solution for scattering from semicircular cylindrical screen [19]. The remainder of the paper will proceed as follows. Section 2 presents a novel method solution to the Dirichlet problem for screens, which converges in L_2 , and permits to estimate directly a magnitude of scattering amplitude error. Section 3 details the method estimation of an actual error of the EFIE solution. Section 4 presents the adequacy verification of the new method. Section 5 presents implementations of this method for testing some practically used MoM algorithms. The final section presents conclusion.

2. THE GALERKIN METHOD FOR E-SCREENS

Let the electric field outside a screen be a sum of an incident field

$$E_0(x, y) = \exp(-jkx \sin i_0 - jky \cos i_0) \quad (1)$$

and a scattered field, which we will seek as a single-layer potential

$$E_{sc}(x, y) = \int_{\partial L} G(x, y, s) \varphi(s) ds. \quad (2)$$

Here, the incidence angle i_0 is counted clockwise from the $-Y$ direction (Fig. 1), k is the free space wave number, and φ is an unknown function, which is proportional to the surface current. The function

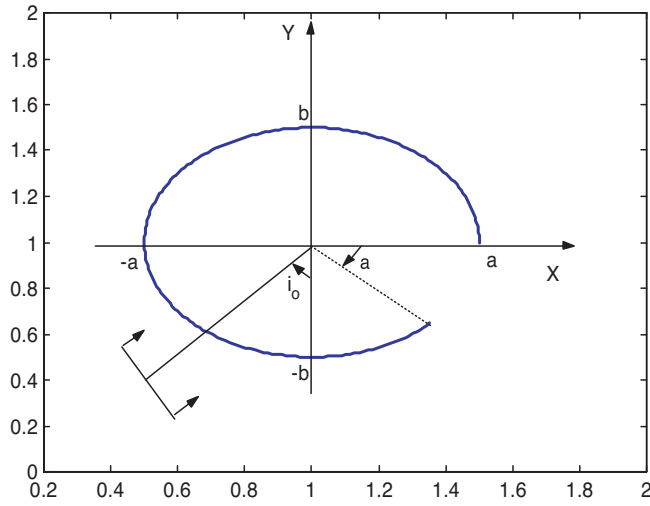


Figure 1. Geometry of the problem.

$$G(x, y, s) = \frac{1}{4j} H_0^{(2)}(kR(x, y, s)) \quad (3)$$

stands for the free space Green's function with

$$R(x, y, s) = \sqrt{(x - x(s))^2 + (y - y(s))^2}$$

and

$$x = x(s), \quad y = y(s), \quad s \in [0, L] \quad (4)$$

being a C^∞ -parameterization of a smooth boundary ∂L of the length L of a screen. Let us go to new parameterization using new variable:

$$\sigma = -1 + 2s/L, \quad \sigma \in [-1, 1]. \quad (5)$$

The scattered field (2) can be then represented as

$$E_{sc}(x, y) = \frac{L}{2} \int_{-1}^1 G(k\bar{R}(x, y, \sigma)) \bar{\varphi}(\sigma) d\sigma \quad (6)$$

with

$$\bar{R}(x, y, \sigma) = \sqrt{(x - \bar{x}(\sigma))^2 + (y - \bar{y}(\sigma))^2}, \quad (7)$$

new parameterization of the boundary ∂L :

$$x = \bar{x}(\sigma) = x(0.5L + 0.5L\sigma), \quad y = \bar{y}(\sigma) = y(0.5L + 0.5L\sigma), \quad (8)$$

and new unknown function $\bar{\varphi}(\sigma) = \varphi(0.5L + 0.5L\sigma)$. The Dirichlet condition yields the EFIE

$$0.5L \int_{-1}^1 G(k\bar{R}(\sigma, \sigma'))\bar{\varphi}(\sigma')d\sigma' = F(\sigma), \quad \sigma \in [-1, 1] \quad (9)$$

when using (6). Here, $F(\sigma) = -E_0(\bar{x}(\sigma), \bar{y}(\sigma))$ and

$$\bar{R}(\sigma, \sigma') = \sqrt{(\bar{x}(\sigma) - \bar{x}(\sigma'))^2 + (\bar{y}(\sigma) - \bar{y}(\sigma'))^2}.$$

It is known that a solution to (9) exhibits the singular behavior $\sim |1 - \sigma^2|^{-1/2}$ at the end points: $\sigma = \pm 1$. This issue prevents from seeking a solution in familiar Hilbert space L_2 . This obstacle can be circumvented with the aid of special change of variable in (9) proposed first in [20]: $\sigma' = -\cos t'$, $t' \in [0, \pi]$. Using this procedure, the Equation (9) can be rewritten as

$$\int_0^\pi H_0^{(2)}(k\tilde{R}(t, t'))\psi(t')dt' = f(t), \quad t \in [0, \pi] \quad (10)$$

with

$$\tilde{R}(t, t') = \sqrt{(\tilde{x}(t) - \tilde{x}(t'))^2 + (\tilde{y}(t) - \tilde{y}(t'))^2}, \quad (11)$$

new unknown function

$$\psi(t) = \frac{L}{8j}\bar{\varphi}(\cos t)\sin t, \quad (12)$$

new parameterization

$$x = \tilde{x}(t) = \bar{x}(\cos t), \quad y = \tilde{y}(t) = \bar{y}(\cos t), \quad (13)$$

and new right-hand side (RHS)

$$f(t) = F(\cos t). \quad (14)$$

It is clear that the new unknown function (12) is nonsingular now at end points ($t = 0, \pi$) despite the mentioned singular behavior of the surface current function $\bar{\varphi}$. The scattered field can be rewritten then as

$$E_{sc}(x, y) = \int_0^\pi H_0^{(2)}(k\tilde{R}(x, y, t'))\psi(t')dt' \quad (15)$$

with

$$\tilde{R}(x, y, t) = \sqrt{(x - \tilde{x}(t'))^2 + (y - \tilde{y}(t'))^2}.$$

Summarizing, we eliminate the singular behavior of a solution to the EFIE for screens and this procedure leads automatically to a new domain of integral equation, viz., $[0, \pi]$. Now we can seek a solution to (10) in L_2 , using the Fourier representation of unknown function

$$\psi(t) = \sum_{n \geq 0} a_n \cos nt. \quad (16)$$

The widely known procedure yields the traditional MoM equation in the space of sequences:

$$Ka = f \quad (17)$$

with matrix elements of K and f :

$$K_{mn} = \int_0^\pi \cos mtdt \int_0^\pi H(t, t') \cos nt' dt', \quad (18)$$

$$f_m = \int_0^\pi f(t) \cos mtdt, \quad (19)$$

and

$$H(t, t') = H_0^{(2)}(k\tilde{R}(t, t')). \quad (20)$$

Prove that this equation can be transformed to a Fredholm one with the aid of equivalent transformations making use of special operator (regularizer) \mathfrak{R} , which has the following matrix elements:

$$\mathfrak{R}_{mn} = \int_0^\pi \cos mtdt \int_0^\pi \overset{\circ}{H}(t, t') \cos nt' dt',$$

with

$$\overset{\circ}{H}(t, t') = -\frac{2j}{\pi} \ln \left| 2e^{-1} (\cos t - \cos t') \right|. \quad (21)$$

These matrix elements can be evaluated analytically making use of the known integral [20, 21]:

$$-\frac{1}{\pi} \int_{-\pi}^{\pi} \ln \left| 2e^{-1/2} \sin \frac{t-t'}{2} \right| e^{jnt'} dt' = \rho_n e^{jnt} \quad (22)$$

with $\rho_n = (\delta_{0n} + |n|)^{-1}$ and δ_{mn} being the Kroneker delta. With the aid of (22), we can obtain the following form of the regularizer:

$$\mathfrak{R}_{mn} = \pi j \frac{1 + \delta_{0m}}{\delta_{0m} + m} \delta_{mn}. \tag{23}$$

Using the operator \mathfrak{R} , we can transform the traditional MoM Equation (17) as follows:

$$\mathfrak{R}a + Ta = f \tag{24}$$

with

$$T = K - \mathfrak{R} \tag{25}$$

having the matrix elements:

$$T_{mn} = \int_0^\pi \cos mtdt \int_0^\pi P(t, t') \cos nt' dt'. \tag{26}$$

Here, the function

$$P(t, t') = H(t, t') - \overset{\circ}{H}(t, t') \tag{27}$$

is nonsingular, and more, $P \in C^\infty(\Omega \times \Omega)$ with $\Omega = [0, \pi]$ for smooth boundary of the mentioned properties. This one can be easily seen from the following representation:

$$P(t, t) = 1 - \frac{2j}{\pi} (1 + C - 2 \ln 2 + \ln ka) - \frac{2j}{\pi} \ln \frac{\Lambda(\cos t)}{a} \tag{28}$$

where $\Lambda(\sigma) = (\dot{x}^2 + \dot{y}^2)^{1/2}$ with pointed quantities being the derivatives of (8) with respect to σ , $C = 0.577\dots$ the Euler constant, and a being a half of maximum size of a scatterer. For $\partial L \in C^\infty$, there exists such an ε , that $\Lambda \geq \varepsilon > 0$, and then $P(t, t) \in C^\infty(\Omega)$, analogously to the static case [20]. Such behavior of the function P permits us to integrate by parts in (26) that, in turn, permits one to prove the decay rate of matrix elements T_{mn} as being $O(m^{-2}n^{-2})$ with harmonic numbers (m and n) increasing. At the same time, both the traditional GMoM matrix elements (K_{mn}) and auxiliary matrix ones ($\overset{\circ}{K}_{mn}$) decay separately only as $O(m^{-1}n^{-1})$. This is the point that permits us to transform the traditional MoM Equation (17) of the first kind to a Fredholm one. To this end, let us apply the operator S^{-1} with matrix elements

$$S_{mn}^{-1} = (1 + m)\delta_{mn} \tag{29}$$

to the both sides of Equation (24). Then, it becomes

$$S^{-1}\mathfrak{R}a + S^{-1}Ta = S^{-1}f, \quad (30)$$

which is no other than a Fredholm equation. It is worthwhile to note that one can also use the inverse operator \mathfrak{R}^{-1} instead of S^{-1} . It is just simpler from theoretical point of view but gives larger condition number when solving this equation numerically. Let us prove that the Equation (30) is Fredholm. Using the decay rate of T_{mn} as being $O(m^{-2}n^{-2})$ and asymptotic behavior of S_{mn}^{-1} as $O(m)$ which follows from (29), we can see that $(S^{-1}T)_{mn} = O(m^{-1}n^{-2})$ and then, the operator $S^{-1}T$ is compact in l_2 . We can easily see that the operator $S^{-1}\mathfrak{R}$ is Fredholm in l_2 as well because its matrix elements can be written as

$$(S^{-1}\mathfrak{R})_{mn} = \pi j(1 + \delta_{0m})\delta_{mn} + \pi j(1 + \delta_{0m})\frac{1 - \delta_{0m}}{\delta_{0m} + m}\delta_{mn}.$$

Here, the first matrix corresponds to an invertable operator, and the second one corresponds to a compact one. Further, according to [22], for existence of a solution to the Equation (30) the RHS vector $S^{-1}f$ has to be square summable. Let us prove that it is really so. Integrating by parts in (19), one can obtain the asymptotic behavior of f_m as $f_m = O(m^{-2})$, and then, using (29): $(S^{-1}f)_m = O(m^{-1})$. Because of that, $S^{-1}f \in l_2$. All these prove that the Equation (30) is Fredholm and has a unique solution if the determinant of the MoM system is nonzero. In this case, as has been proved in [23], $a \in l_2$ and the approximate solution

$$\psi_N(t) = \sum_{n=0}^N a_n \cos nt \quad (31)$$

converges to an exact solution of integral Equation (10) in L_2 . The uniqueness of a solution is guaranteed by the determinant of K_{mn} , and hence of $(S^{-1}\mathfrak{R} + S^{-1}T)_{mn}$, being nonzero. Let us prove this issue. As has been proved in [24], the homogeneous integral Equation (10) has trivial solutions only. Because of that, the corresponding integral operator has no eigenvalue that equals to zero. Further, because of the spectrum of integral operator in (10) coincides with that of its discretized counterpart (17), and hence (30), if we use the Galerkin method [23], the determinant of the system in (17), and hence in (30), is nonzero. All these prove the convergence of the Galerkin MoM solution to the EFIE in L_2 .

Summing, it is worthwhile to note that trivial operation of adding and subtracting the regularizer \mathfrak{R} from the main operator K in (24)

leads to completely nontrivial result exclusively due to using of a complete set of trigonometric functions as bases functions and general property of the Fourier integrals. Due to the latter one, the more smoother is the integrand of a Fourier integral (P in (26)) the more fast diminish the matrix elements T_{mn} . It is namely this issue that permits one to obtain a Fredholm matrix equation for modal coefficients instead of the common MoM equation with a compact matrix operator.

3. ACTUAL ERROR

One of the main problems of the EFIE solving procedure is the estimation of an actual error of an approximate solution with the aid of residual error computed in L_2 . The latter stands for the boundary condition's error and can be easily computed in practice. This problem has been considered in [1–5] in the energy Sobolev space. However, actual error estimation has been obtained in the form, which does not permit to obtain a magnitude of actual error if we know a magnitude of discrepancy. Recently, authors solved this problem in familiar L_2 space for closed cylinders [16, 17] and H -screens [18]. Here, we consider this problem for E -screens.

The completeness of basis functions used permits us to obtain a rigorous relationship between actual and residual errors. To this end, let us write down an actual error as a function

$$\varepsilon(t) = \psi(t) - \psi_N(t). \quad (32)$$

One can easily see that this function satisfies the integral equation

$$\int_0^\pi H(t, t') \varepsilon(t') dt' = d_N(t), \quad t \in \Omega \quad (33)$$

where

$$d_N(t) = f(t) - \int_0^\pi H(t, t') \psi_N(t') dt' \quad (34)$$

is a residual error function. Let us derive the actual error function from (33). This equation is exactly the same as (10) except the RHS. As is clear from the above, the developed Galerkin MoM procedure for solving the Equation (33) converges if the RHS function (34) is continuous on Ω . It is really so. The first addend in (34) is obviously continuous. The second one is continuous as well because it is a single-layer potential. Hence, we can use the abovementioned technique to

obtain a convergent MoM solution for the error function

$$\varepsilon(t) = \sum_{n \geq 0} \alpha_n \cos nt \quad (35)$$

in L_2 . As is clear from (30), the corresponding solution in l_2 for the Fourier coefficients can be written then as

$$\alpha = (S^{-1} \overset{\circ}{K} + S^{-1}T)^{-1}D, \quad (36)$$

where vector D has the coordinates

$$D_m = (1 + m) \int_0^\pi d_N(t) \cos mtdt. \quad (37)$$

Because $d_N(t)$ is continuous and its derivative is integrable, one can easily prove by integrating by parts that integral in (37) decays asymptotically as m^{-2} with m . Then, $D_m = O(m^{-1})$ and hence, $D \in l_2$. This is sufficient for the Galerkin MoM convergence in L_2 , and this one permits us to use the Parseval equality

$$\|\varepsilon\|_{L_2} = \|\alpha\|_{l_2},$$

which permits one to relate the actual and residual errors in the form of

$$\|\psi - \psi_N\|_{L_2} = \|(S^{-1}\mathfrak{R} + S^{-1}T)^{-1}D\|_{l_2}, \quad (38)$$

if we account for (32), (34), (36), and (37).

4. NUMERICAL RESULTS

A. E (TM) – case

Noting that a suitable reference solution for testing practically used MoM algorithms in L_2 is not found to date, we give here the adequacy verification of the presented Galerkin MoM that can be used as such a reference solution. To this end, we use the canonical geometry of a circular screen. Such a canonical problem has been solved semi-analytically with the aid of the Riemann-Hilbert technique developed in [19, 25]. The Riemann-Hilbert technique solution we use in the form outlined in [25] with the aid of the computational code pleasantly given us by one of the authors of this paper. The excellent agreement between the two solutions is demonstrated in Fig. 2. The both solutions are within 0.1% *rms* error for the considered case when the scattering plane

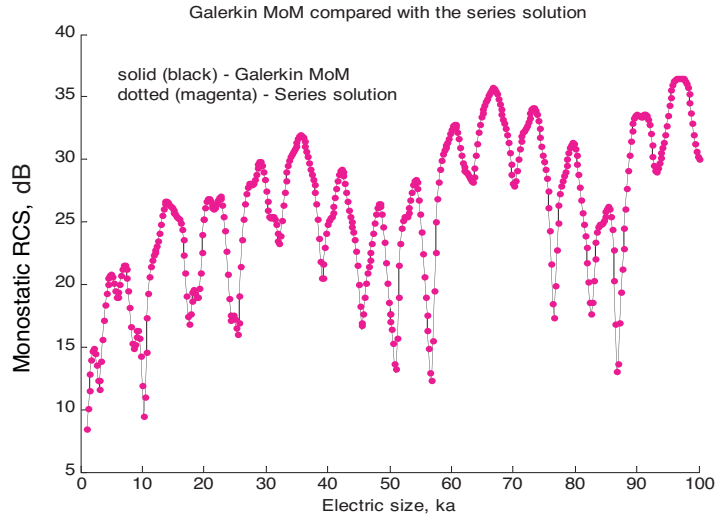


Figure 2. Monostatic RCS for scattering from semicircle screen computed with the aid of the Galerkin MoM (solid curve) and series solution [14] (dotted curve) within 0.1% *rms* error if the scattering plane E -wave impinges normally on the slot ($i_0 = 0$).

E -wave impinges normally on the slot ($i_0 = 0$). Presented investigation and favorable comparison of results, permits us to be sure in adequacy of the reference solution.

With the new reference solution in hand, we investigate the widely used MoM algorithms, viz., that in which the collocation points are shifting from the nodal points (MoM with PS), and that in which the singular integrals are evaluated more rigorously with the aid of the singularity extraction method [26] (MoM with SE), for solving E -scattering from screens. The first algorithm is more economical because it requires not any efforts the logarithmic singularities to overcome. Naturally, it is less accurate than more complex algorithm, the MoM with SE, with exact evaluation of singular integrals, but it is interesting to what degree? Such a question to answer, we investigate the mentioned MoM algorithms with the aid of the proposed reference solution. We are interesting here in the scattering amplitude *rms* error diminishing rate (as in [9]) and error dependence on the incidence angle. The latter issue was pointed out in [9], and arises from the dependence of surface current behavior along the scatterer on the incidence angle. We demonstrate in Fig. 3 the current function features for two specific incidences, frontal and oblique, for the strip, semicircle

screen and right triangle screen, all of electric size 10. Graphics show that current function oscillates more rapidly for frontal incidence, and hence the *rms* scattering amplitude error may be larger in this case than that for oblique incidence.

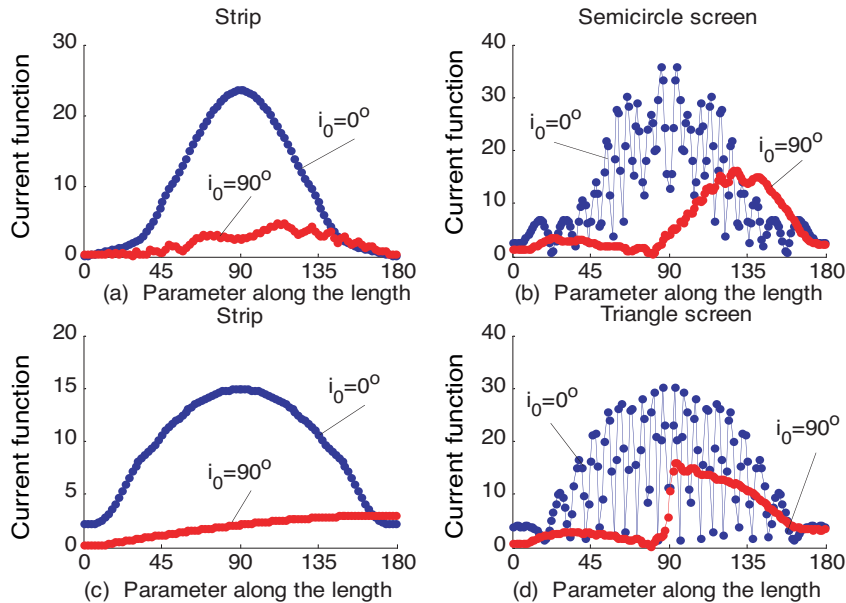


Figure 3. Current function in the RS within 0.1% actual error for $ka = 10$ and mesh density 30. (a) strip as a degenerated elliptic screen; (b) semicircle screen; (c) strip as a degenerated triangle screen; (d) right triangle screen.

The scattering amplitude *rms* error diminishing rate for the MoM with PS we demonstrate in Fig. 4 for the semicircle screen and strip of electric size 10, for frontal and oblique incidence. With the aid of the reference solution, we investigate here the diminishing rate of the angle-averaged scattering amplitude error (dotted curve) and the discrepancy of the MoM-with-PS solution (asterisked curve). We see that for this algorithm the discrepancy behavior is very close to that of scattering amplitude error, but the magnitude of discrepancy is far less than that of scattering amplitude error. Because of that, the estimation of a MoM algorithm's accuracy with the aid of discrepancy may give a significant error. It is worthwhile to note that, as has been noted in [9], the rate of diminishing does not depend practically on the incidence angle but it is not so for an error magnitude. Particularly, this issue is most noticeable for strip.

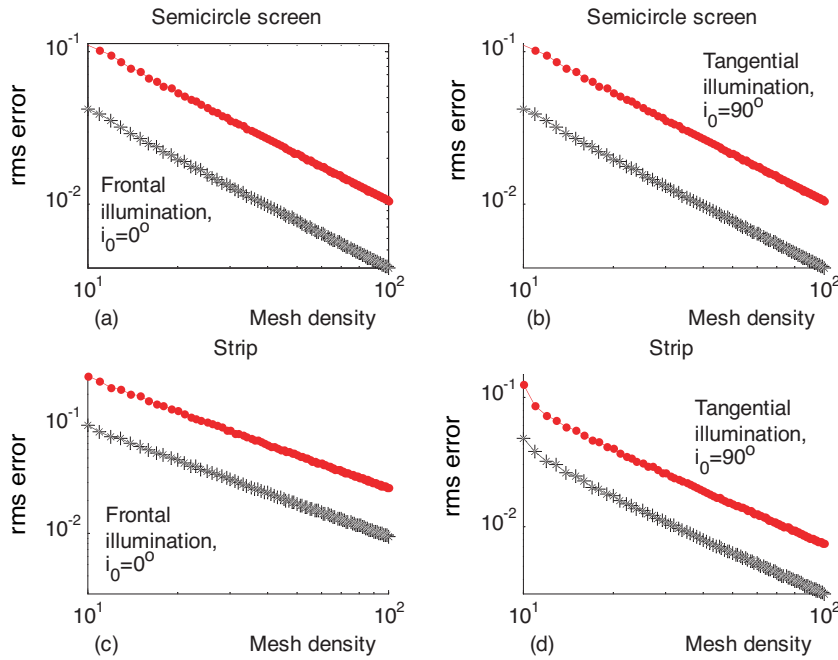


Figure 4. Scattering amplitude *rms* error diminishing rate of tested MoM algorithm, viz., the Galerkin collocation on pulse basis with nodal points shifting, computed by comparing with the reference solution (RS). For the tested MoM: dotted curve — the angle-averaged scattering amplitude *rms* error; asterisked curve — discrepancy of the MoM solution. The both scatterers are of electric size 10.

Analogous investigations have been provided for the MoM-with-SE, where singular integrals have been calculated more exactly with the use of the singularity extraction method (SE), [26]. The results are shown in Fig. 5. We see here the more substantial dependence of scattering amplitude error magnitude on the incidence angle, and drastically difference between the scattering amplitude *rms* error diminishing rate and discrepancy rate, particularly for the strip, graphics (c)–(d). This issue and that of obtained above shows that one would not use the discrepancy as an estimate of scattering amplitude error for any MoM algorithm in the L_2 function space.

Consider now the most important practical question of how to use the reference solution obtained for picking out the needed mesh density for commonly used MoM algorithms in L_2 . This really may be done if we account for the independence of scattering amplitude error

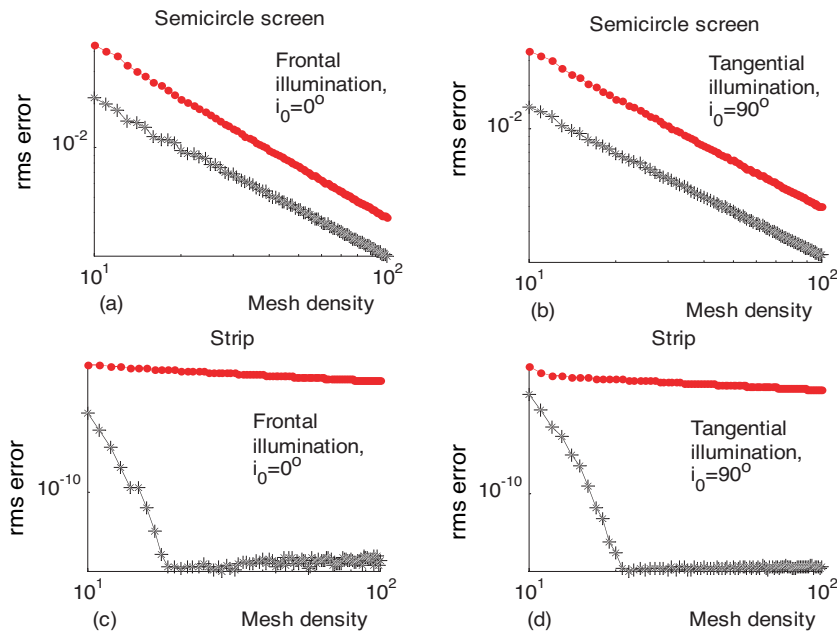


Figure 5. Scattering amplitude *rms* error diminishing rate of tested MoM algorithm, viz., the Galerkin collocation on pulse basis with exact evaluating of singular integrals, computed by comparing with the reference solution (RS). For the tested MoM: dotted curve — the angle-averaged scattering amplitude *rms* error; asterisked curve — discrepancy of the MoM solution. The both scatterers are of electric size 10.

diminishing rate from the frequency of scattered field (or equally, from the electric size of a scatterer) mentioned in [9]. This one means that if we calculate the scattering amplitude error of any MoM algorithm in L_2 for any mesh density with the aid of the RS at moderate frequencies, the difference between errors will be the same at high frequencies. If, additionally, the errors' magnitudes are independent from the field frequency as well, we can forecast the MoM algorithm's accuracy at the microwave range by simulating procedure carried out at moderate frequencies.

As for the independence of scattering errors from field frequency, we can note that if not accounting for the possible wrong evaluation of functions used in the MoM algorithm, there is only one cause that can increase the errors at high frequencies. This one is the increasing of condition number of a MoM matrix in l_2 space with electric size of

scatterer. The physical cause of this effect has been outlined in [6–10]. To eliminate the influence of this point, one can use the special iterative methods solution of MoM matrix equations. If so, we can reckon that the scattering errors are independent from the frequency of incident wave.

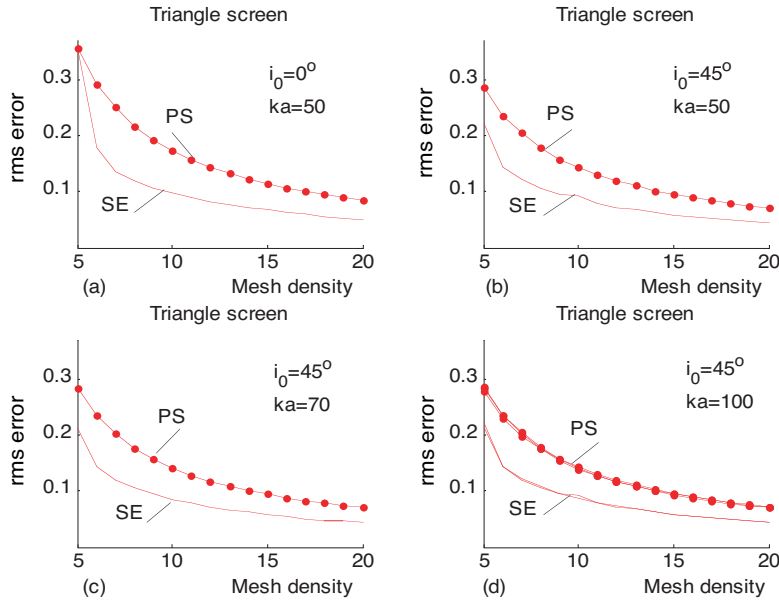


Figure 6. Comparing of the two MoM algorithms with respect of their accuracy for scattering from the right triangle screen of electric size 50 for frontal incidence ($i_0 = 0^\circ$) and incidence on the rib ($i_0 = 45^\circ$), which permits to choose the appropriate MoM algorithm for a given accuracy at microwave range by testing the algorithm for moderate scatterer's electric size ($ka = 50$), graphics (a) and (b). Graphics (b), (c) and (d) demonstrate the independence of the scattering amplitude error form the electric size of a scatterer. In the (d) all three curves (for $ka = 50, 70, 100$) are overlapped to exhibit this issue.

This issue is demonstrated in Fig. 6, where we consider the scattering from the right triangle screen of moderate electric size 50 for two incidence angles: $i_0 = 0^\circ$ (frontal incidence) and $i_0 = 45^\circ$ (incidence on the rib). Scattering amplitude *rms* errors calculated by comparing to the RS for some values of the mesh density (5–20) are exhibited in this figure for two MoM algorithms (with PS and with SE) with the goal of demonstrating the possibility of

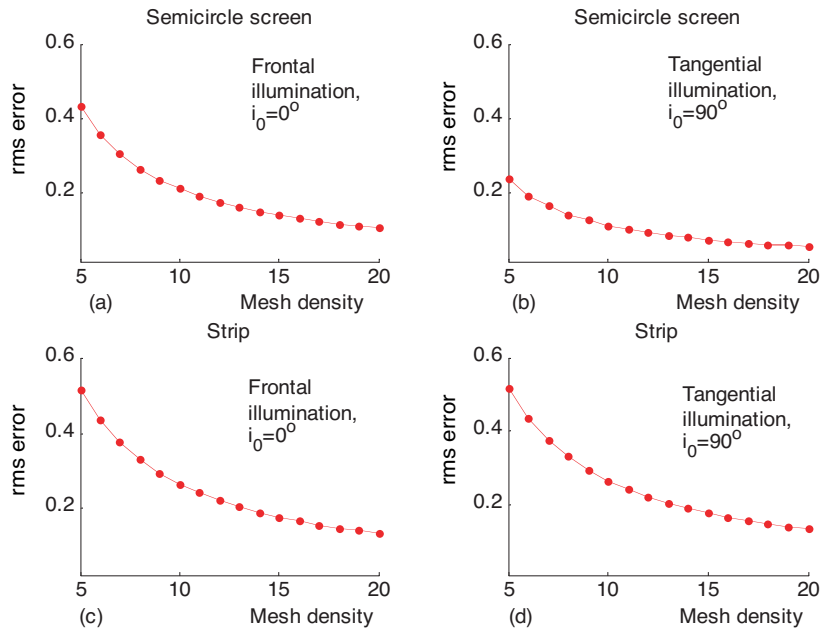


Figure 7. Scattering amplitude *rms* error behavior for the tested MoM algorithm — the MoM with PS, which permits to choose the needed mesh density for a given accuracy at microwave range by testing the algorithm for moderate scatterer’s electric size ($ka = 50$).

choosing the appropriate mesh density for these two at the microwave range (graphics (a), (b)). In the same figure, we demonstrate the independence of errors from the electric size of the scatterer (graphics (b)–(d)). To this end, all three curves, namely for $ka = 50, 70$, and 100, are overlapped in (d) for each MoM algorithm. As we can see from all these, the errors really are practically independent from ka and this one gives the opportunity of appropriate choosing the mesh density for achieving needed accuracy of tested MoM algorithms. Thus, analyzing the scattered field errors for specified configuration and various incidence angles, one can choose the appropriate mesh density, which may be far less than that given by the commonly used rule of “ten points on the wavelength”. It is worthwhile to note that the ten-points-mesh has no remarkable features, which could justify its wide implementation in practice, as we can see in Fig. 6 and further. For judiciously choosing of a mesh density for any MoM algorithm, one would investigate carefully the scattering errors for some specific geometries. For 2-D screens, such specific configurations

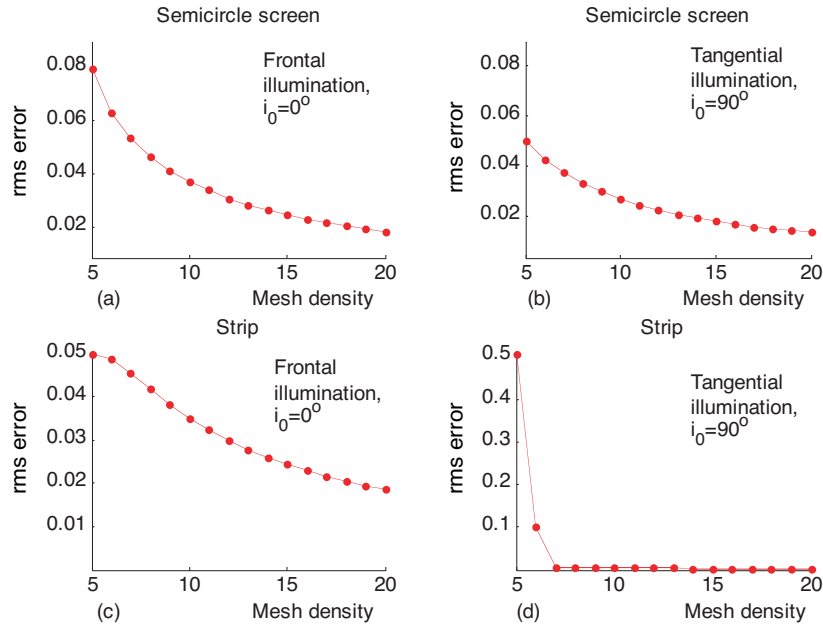


Figure 8. Scattering amplitude *rms* error behavior for the tested MoM algorithm — the MoM with SE, which permits to choose the needed mesh density for a given accuracy at microwave range by testing the algorithm for moderate scatterer’s electric size ($ka = 50$).

would be: a right triangle screen, a semicircular screen and a strip. Error behaviors for the last two are shown in Fig. 7 for the MoM with PS, and in Fig. 8 for the MoM with SE. All these graphics permit to choose judiciously the appropriate mesh density by carrying out the simulations at moderate frequencies and extrapolate obtained results to the microwave range.

B. H (TE) – case

A rigorous Galerkin solution in L_2 for scattering of an H -polarized plane wave by a 2-D screen has been developed in [18]. As for the E -case, this solution can be used as a reference solution (RS) for testing MoM algorithms in L_2 , commonly used in practice for simulating H -scattering from screens. To demonstrate such possibilities, we investigate the MoM algorithm with triangle expansion and testing functions [27], in which the hypersingular integrals are evaluated as a finite part in the sense of Hadamard with the aid of special quadrature

formula. Using the RS, we calculate the scattering amplitude *rms* error for scattering from semicircular screen of electric size 10 for some specific incidence angles. With these calculations in hand, we investigate the scattering amplitude error diminishing rate for this MoM algorithm. Its dependence on the incidence angle can be noticed in Fig. 9, too. As for the *E*-case (Fig. 5), we see that in the *H*-case the scattering amplitude error diminishing rate may be not the same as that for discrepancy, and hence the latter should not be used as a performance of accuracy of any MoM algorithm in L_2 as well. Noting that there is no appropriate reference solution to date for computer simulation of *H*-scattering from screens, the RS obtained in this paper gives the only opportunity to estimate the scattering amplitude error of any MoM algorithm in L_2 and choose an appropriate mesh density for parsimonious calculations. The latter can be done exactly in the same manner as that for the *E*-case outlined above.

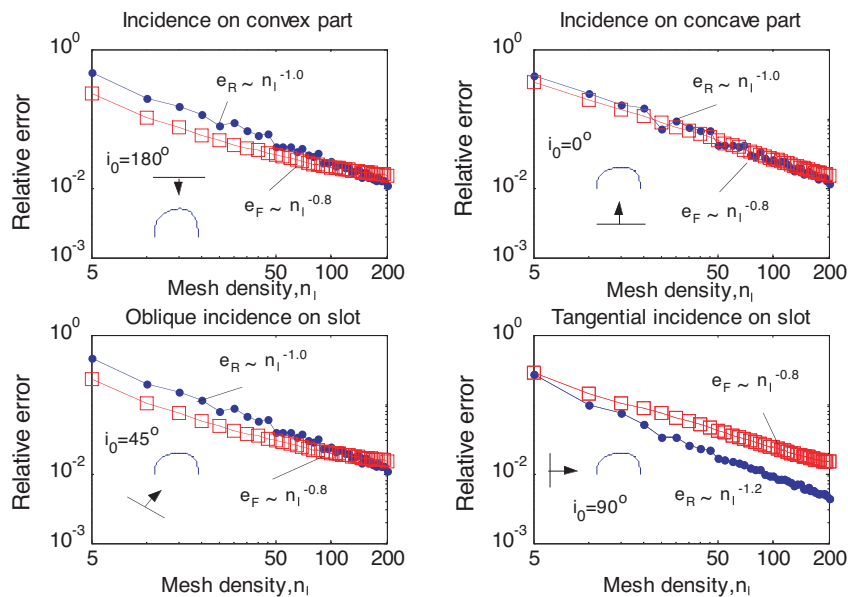


Figure 9. Scattering amplitude *rms* error diminishing rate of tested MoM algorithm for *H*-scattering from semicircular screen, viz., the MoM on triangle basis with evaluating of singular integrals in the sense of Hadamard, computed by comparing with the reference solution (RS). For the tested MoM: squared curve — the angle-averaged scattering amplitude *rms* error; dotted curve — discrepancy of the MoM solution. The scatterer is of electric size 10.

5. CONCLUSION

A rigorous Galerkin MoM solution for scattering from E -screens, convergent in L_2 , which permits to estimate the magnitude of an actual error, and, hence, a scattering amplitude error, with the aid of evaluated discrepancy, has been proposed as a reference solution for testing practically used MoM algorithms in L_2 . Comparing tested algorithm with the RS, practitioner can estimate the scattering amplitude error and its diminishing rate with mesh density and electric size of scatterer. The proposed method simulation is more cheap and convenient than widely used methods of experimental benchmarking, and more correct than methods based on comparing with physical optics approximation, or with the same but high mesh density MoM solution.

Using the reference solution obtained in this paper for E -case and previously for H -case, practitioner can investigate not only the scattering amplitude error convergence of the MoM algorithm used, but additionally choose an appropriate mesh density which may be far less than the common used ten points on the wavelength.

REFERENCES

1. Hsiao, G. C., R. E. Kleinman, R. X. Li, and P. M. van den Berg, "Residual error — a simple and sufficient estimate of actual error in solutions of boundary integral equations," *Computational Engineering with Boundary Elements*, Vol. 1: *Fluid and Potential Problems*, S. Grill, C. A. Brebbia, and A. H. D. Cheng (eds.), 73–83, Computational Mechanics Publ., Boston, MA, 1990.
2. Hsiao, G. C. and R. E. Kleinman, "Feasible error estimates in boundary element methods," *Boundary Element Technology VII*, C. A. Brebbia and M. S. Ingber (eds.), 875–886, Computational Mechanics Publ., Boston, MA, 1991.
3. Van den Berg, P. M., A. P. M. Zwamborn, G. C. Hsiao, and R. E. Kleinman, "Iterative solutions of first kind integral equations," *Direct and Inverse Boundary Value Problems*, R. E. Kleinman, R. Kress, and E. Martensen (eds.), 213–232, Lang, Frankfurt, Germany, 1991.
4. Hsiao, G. C. and R. E. Kleinman, "Error analysis in numerical solution of acoustic integral equation," *Int. J. Numer. Meth. Eng.*, Vol. 37, 2921–2933, 1994.
5. Feistauer, M., G. C. Hsiao, and R. E. Kleinman, "Asymptotic and *a posteriori* estimates for boundary element solutions of

- hypersingular integral equations,” *SIAM J. Numer. Anal.*, Vol. 33, 666–685, Apr. 1996.
6. Warnick, K. F. and W. C. Chew, “Accuracy and conditioning of the method of moments for the 2D EFIE,” *Proceedings of the Annual Review of Progress in Applied Computational Electromagnetics*, 198–204, Naval Postgraduate School, Monterey, CA, March 15–20, 1999.
 7. Warnick, K. F. and W. C. Chew, “Convergence of moment method solutions of the EFIE for a 2D open cavity,” *Microw. Opt. Tech. Lett.*, Vol. 23, 212–218, Nov. 1999.
 8. Warnick, K. F. and W. C. Chew, “Accuracy of the method of moments for scattering by a cylinder,” *IEEE Transactions on Microwave Theory and Techniques*, Vol. 48, 1652–1660, Oct. 2000.
 9. Warnick, K. F. and W. C. Chew, “Error analysis of the moment method,” *IEEE Antennas and Propagation Magazine*, Vol. 46, 38–52, Dec. 2004.
 10. Davis, C. P. and K. F. Warnick, “Error analysis of 2-D MoM for MFIE/EFIE/CFIE based on the circular cylinder,” *IEEE Trans. Antennas and Propag.*, Vol. 53, 321–331, Jan. 2005.
 11. Tyzhnenko, A. G., “Two-dimensional TE-plane wave scattering by a dielectric loaded semicircular trough in a ground plane,” *Electromagnetics*, Vol. 24, 357–368, June 2004.
 12. Tyzhnenko, A. G., “A unique solution to the 2-D H-scattering problem for a semicircular trough in a PEC ground plane,” *Progress In Electromagnetics Research*, PIER 54, 303–319, 2005.
 13. Hongo, K. and Q. A. Naqvi, “Diffraction of electromagnetic wave by disk and circular hole in a perfectly conducting plane,” *Progress In Electromagnetics Research*, PIER 68, 113–150, 2007.
 14. Anastassiou, H. T., “Error estimation of the Method of Auxiliary Sources (MAS) for scattering from an impedance circular cylinder,” *Progress In Electromagnetics Research*, PIER 52, 109–128, 2005.
 15. Hussein, K. A., “Fast computational algorithm for EFIE applied to arbitrarily shaped conducting surface,” *Progress In Electromagnetics Research*, PIER 68, 339–357, 2007.
 16. Tyzhnenko, A. G., “Convergent Galerkin MoM solver for the EFIE in two dimensions,” *Electromagnetics*, Vol. 25, 217–229, Apr. 2005.

17. Tyzhnenko, A. G. and Y. V. Ryeznic, "Convergent Galerkin MoM solution to the hypersingular 1st kind integral equation for 2-D Neumann problem," *Journal of Applied Electromagnetism*, Vol. 6, No. 2, 37–51, 2004.
18. Tyzhnenko, A. G. and Y. V. Ryeznic, "Convergent Galerkin MoM solution for 2-D H-scattering from screens," *Electromagnetics*, Vol. 25, 329–341, May 2005.
19. Colak, D., A. I. Nosich, and A. Altintas, "Radar cross-section study of cylindrical cavity-backed apertures with outer or inner material coating: The case of E -polarization," *IEEE Trans. Antennas and Propag.*, Vol. 41, 1551–1559, Nov. 1993.
20. Yan, Y. and I. H. Sloan, "On integral equations of the first kind with logarithmic kernels," *J. Integral Eq. and Appl.*, Vol. 1, No. 4, 549–579, 1988.
21. Atkinson, K. E., "A discrete galerkin method for first kind integral equations with logarithmic kernel," *J. Integral Eq. and Appl.*, Vol. 1, No. 3, 343–363, 1988.
22. Von Koch, H., "Sur un theoreme de hilbert," *Mathem. Ann.*, Vol. 69, 266–283, 1910.
23. Mikhlin, S. G., *Direct Methods in Mathematical Physics*, Moscow, 1950 (in Russian).
24. Il'iinskiy, A. S. and Y. G. Smirnov, "Integral equations for problems of wave diffraction at screens," *Sov. J. Communicat. Tech. Elect.*, Vol. 39, No. 4, 129–136, 1994.
25. Koshikawa, S., D. Colak, A. Altintas, K. Kobayashi, and A. I. Nosich, "A comparative study of RCS predictions of canonical rectangular and circular cavities with double-layer material loading," *IEICE Trans. Electron.*, Vol. E80-C, No. 11, 1457–1466, Nov. 1997.
26. Sladek, V. and J. Sladek (eds.), *Singular Integrals in Boundary Element Method*, Computational Mechanics Publications, Southampton, U.K., 1998.
27. Morita, N., N. Kumagai, and J. R. Mautz, *Integral Equations Methods for Electromagnetics*, Artech House, London, 1990.